

A Physical Basis for NEXRAD Data Update Rates

Pravas R Mahapatra* and Dusan S Zrnic†

National Severe Storms Laboratory, Norman, Oklahoma

The Next Generation Weather Radar (NEXRAD) is slated to play an important role in the integrated and automated air traffic control system being currently planned by the Federal Aviation Administration. One major point of debate is the minimum rate at which weather data collected by NEXRAD must be updated so that no phenomena potentially hazardous to aviation go undetected. This paper presents the methodology and results of a study to estimate the lifetimes of significant features in typical storm phenomena for situations other than takeoff or landing. These results are of direct relevance in deciding NEXRAD system data update rates. Two methods are used for the lifetime study: photo interpretive and computer based correlation. Several storms are studied using both methods. It is found that the storms studied contain no feature that might have been missed by a 5-min scan cycle provided that concurrent reflectivity, radial velocity, and Doppler spectrum width data at several elevations are utilized in the detection of hazardous phenomena.

Introduction

THE integrated and automated air traffic control (ATC) system being currently planned by the Federal Aviation Administration (FAA) envisages the routine use of weather radar data for enhancing flight safety.¹ The Next Generation Weather Radar (NEXRAD) will thus form an important sensor in the future ATC network. Since the NEXRAD system is being designed for use by several agencies, its parameters require careful balancing of demands that are often conflicting. Among these is the rate (or, equivalently, time interval) of data update.

Present plans for providing weather information to aviation call for en route surveillance with a NEXRAD radar and, most likely, a dedicated NEXRAD type radar at or near airports with a suitable scan rate dictated by the lifetimes of low level hazardous features. Our study and data base do not address this latter application. Specifically, we do not examine the low level wind shear that is a threat at takeoff or landing; so we limit ourselves to the hazards that may be encountered at high altitudes and can be monitored with either an airborne or ground based radar.

In a typical radar application, data concerning the status of weather within the radar range are refreshed at intervals corresponding to a complete scan cycle of the antenna. There are considerable advantages, both from mechanical and signal processing points of view, to having a relatively slow azimuthal scan rate. In addition, if adequate volume coverage requires sampling at a large number of elevation angles, the total scan cycle time tends to be large. However, too infrequent volume data update may result in the radar failing to detect phenomena that grow or decay rapidly (i.e., with time scales shorter than the scan cycle time). Thus, the persistence, or the lifetime, of atmospheric features that are potentially hazardous to aviation, is a physical factor that sets the upper limit on the interval between successive data updates.

The importance of data concerning the lifetime of features in deciding the NEXRAD data update rate has been well recognized.² This paper reviews the various factors influencing the scan cycle time of Doppler weather radars and presents the results of a study conducted recently at National Severe Storms Laboratory (NSSL) on the lifetimes of hazardous weather features. A data update interval of 5 min has been suggested in the NEXRAD context by many potential user agencies, but there are certain reservations as to whether such a rate would be adequate in the case of aviation weather surveillance in the en route environment or whether it would be necessary to speed up the update rate by, say, a factor of 2. This problem is continually addressed during the course of the paper.

Past studies on lifetimes of weather features³ using radar observations have principally relied on reflectivity data only. This is because operational weather radars and most research radars in the past have had little capability beyond the measurement of the intensity of weather echo returns. NSSL has built up an advanced signal processing facility in which the signals received by a 10 cm Doppler radar are processed in real time to yield reflectivity (precipitation), radial velocity (windspeeds, large scale shear), and spectral width (small-scale shear and turbulence) data over the entire volume of observation. Using these data, it is possible to analyze more aspects of a weather feature than did earlier studies.

Spatial correlation, described later in this paper, is a convenient method of quantitatively estimating the lifetimes of atmospheric features. In the past, this technique has been applied typically for studying internal motions within storm fields^{4,5} and for determining statistical properties of weather echoes.⁶ At NSSL, this method has been applied to study the time decay of the correlation function of clear air turbulence and to retrieve the crosswind components from single Doppler radar data.⁷ As a byproduct of the above correlation studies, limited results are available^{5,7} on feature persistence. Recently, the correlation algorithm has been refined and expanded to handle multimoment data and variable feature size and number.

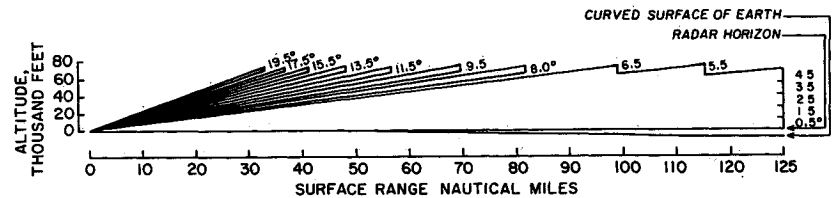
Earlier results available at NSSL also include data on persistence of gust fronts. These data seem to indicate that gust fronts have a fairly high order of stability (>40 min) and, hence, have little danger of being missed in any practical scan cycle. Attention is therefore focused in this paper on the lifetimes of features within thunderstorms capable of possessing fast growth and decay rates.

Received Aug 4 1983; revision received April 1 1984. This paper is declared a work of the U.S. Government and therefore is in the public domain.

*Visiting Research Associate, Cooperative Institute for Mesoscale Meteorological Studies, University of Oklahoma. On leave from Department of Aerospace Engineering, Indian Institute of Science, Bangalore, India.

†Leader of the Doppler Radar Project.

Fig 1 Suggested set of scan levels for NEXRAD system



Radar Detection of Aviation Weather Hazards

Atmospheric convection can pose hazards to aviation and cause flight discomfort and delays, as well as uneconomic airline operation.^{8,10} The types of phenomena potentially hazardous to aviation are well documented.^{11,12} Heavy precipitation (rain and hail), severe turbulence, and vortices are hazardous to flight at all altitudes. In addition, low level windshears, small but intense downdrafts, are known sources of aviation hazard during low level flight at takeoff and landing, but these will not be examined in this study.

A conventional weather radar provides a volume coverage of precipitation out to a range of a few hundred kilometers. If the radar has coherent measurement or "Doppler" capability,¹³ then the radial components of windspeed and turbulence and/or shear can be observed in addition to reflectivity (which corresponds to intensity of precipitation) over the observation volume.

For several well known reasons a weather radar must operate in a pencil beam mode. Beam widths usually employed are of the order of a degree. For wider coverage, the beam must scan the volume of space that is to be observed. The usual scanning scheme, and one that will most likely be adopted for NEXRAD, consists of rotating the antenna continuously in azimuth over a full circle (or a sector) and discretely incrementing the elevation between successive azimuth scans. The considerations for deciding these parameters are discussed in the following section.

Constraints on the Scan Cycle

Several considerations, practical as well as theoretical, impose constraints on the scan cycle of a weather radar. A proper understanding of these factors is necessary for deciding a scan strategy for NEXRAD radars in their role as detectors of convective phenomena hazardous to aviation.

The limits of the azimuth sector to be scanned by a weather radar are decided by the requirement that the sector must cover the area or phenomenon of interest. For general weather monitoring, such as that conducted by the National Weather Service, the azimuth scan usually covers a full circle. To observe specific features, such as mesocyclones, from a distant point, a sector scan may be sufficient. The NEXRAD system, which is being designed with a broad weather application in mind, is expected to have a full circular scan at most installations. Thus, although in specific situations a sector scan may be advantageous, a circular scan is assumed for the purpose of the present study.

The elevation increments are constrained by the spatial sampling requirements at maximum range. This in turn, is governed by the vertical structure of the phenomena of interest. In the present context, the spatial sampling should be fine enough so as not to miss hazardous phenomena through undersampling. The incremental elevation need not be constant over the entire elevation interval, but may be varied to suit the vertical scale of features at different altitudes and the fact that a feature of a given size subtends a larger angle at closer ranges. Such variations may also be introduced to keep the scan cycle time within reasonable limits. The suggested scan levels for NEXRAD are shown in Fig 1.

The highest elevation to be covered by a weather radar depends on the maximum height to which hazardous phenomena must be observed and the minimum range at

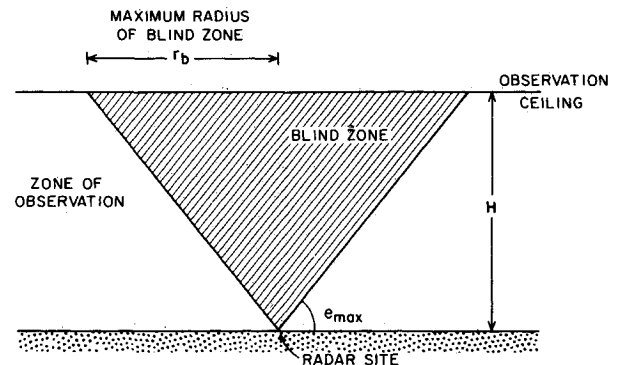


Fig. 2 Geometry of radar blind zone

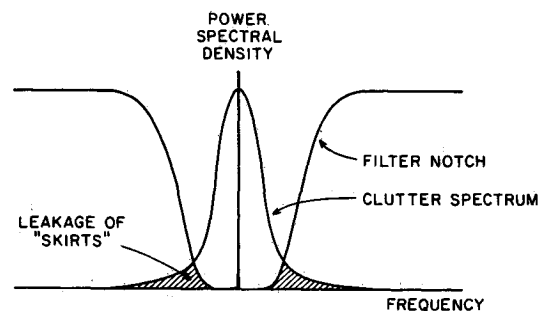


Fig. 3 Schematic showing clutter leakage through notch filter

which such observation must be made. The former can be determined by studying various types of convective phenomena and determining the maximum height up to which hazardous levels of air currents, turbulence, or precipitation may occur. The minimum range at which storms should be "topped" is a matter of choice and compromise. It would be ideal to be able to observe the tops of storms down to near zero range, but the resulting hemispherical scan volume would require a long scanning time. It is customary to limit the highest elevation angle to a value much less than 90 deg and accept a certain "blind zone" as a consequence. The largest radius of the blind zone r_b , is given as (see Fig 2)

$$r_b = H_{\max} \cot e_{\max} \quad (1)$$

where H_{\max} is the maximum height to be observed and e_{\max} is the highest elevation angle of radar antenna. More discussion about scanning time follows later.

The angular speed of the antenna in azimuth is a more complex parameter to determine than the previous three. The rotational speed is based on several considerations:

1) Mechanical. The motor drive and control tend to be more expensive as the rotational speed increases for a given antenna size. Also, there is a higher energy requirement and reduced bearing life at higher speeds. Thus, from a purely mechanical viewpoint, a slower antenna speed is preferable.

2) Signal processing. Coherent signal processing requires the returns from more than one transmitted pulse for

estimating mean velocity and spectral width. The estimation accuracy of spectral moments increases monotonically with the number of samples processed.¹⁴ Typically, 64, 128 or 256 samples are used for moment estimation, the higher numbers being necessary under very poor signal to noise situations especially if ground clutter interference is severe, requiring extensive filtering. Antenna rotation during the period of sample collection causes an effective broadening of the beam pattern¹⁵ resulting in "blurring" or loss of resolution the more the number of samples to be processed, the slower must be the antenna rotation. Thus, weaker weather targets, such as clear air phenomena, would favor a slower scanning speed.

Another important signal processing aspect favoring slow scan is the broadening of ground clutter spectrum due to antenna rotation. Nearly all efficient frequency domain filtering techniques to remove ground clutter^{16,17} are based on the premise that the clutter spectrum is confined to a very narrow band centered on the zero frequency line, whereas weather echoes are centered at mean Doppler frequencies typically removed from zero. In such a case, the clutter filter is of band rejection type with a deep notch coinciding with the dc line. A fast antenna scan rate causes the clutter spectrum to widen and its "skirts" tend to leak past the band rejection filter (Fig 3). To minimize this leakage the filter notch would have to be much wider than the clutter spectrum, resulting in significant loss of information from the weather spectrum. Thus, the consideration of clutter spectral spread also favors a slow rate of antenna scan. This would be particularly necessary at very low elevation angles where ground clutter causes strong interference.

3) Data update rate. During the time taken by the radar antenna to complete a cycle of scan, spectral moments of each resolution cell are obtained once. This assumes that signal processing is done in real time. The longer the scan period of a radar, the larger is the interval at which the meteorological status of the scan volume is sampled, i.e., the slower the data update rate. However, sampling the weather data should not be so slow that atmospheric features may grow to potentially hazardous levels and/or decay out of existence in the period between scans.

The total scan time depends on the width of the sector being scanned, the scan rate, and the number of elevation steps in

the scan cycle:

$$S = \psi n / \omega + \Delta S \quad (2)$$

where S is the total scan time in seconds, ψ the azimuth sector width in degrees, ω the antenna rotation rate in deg/s, n the number of elevation steps in the scan cycle, and ΔS the sum total of braking and reversal times at the end of each sector scan and transition times between elevation angles. If the azimuth scan is over a full circle as is usually the case with weather surveillance, ψ equals 360 and then the scan time depends only on the angular scan rate and the number of elevation steps:

$$S = 360n / \omega + \Delta S \quad (3)$$

If the scan time is decided from physical considerations such as the properties of the weather field, a slow scan rate would force the number of scan levels to be reduced, which makes the spatial sampling coarse. To achieve a finer spatial sampling a higher scan rate must be employed.

The various influences on scan rate and cycle time may be summarized as follows: There are overwhelming system considerations in a weather radar to favor a slow scanning rate. The major factors forcing a speeding up of the scanning process come from the characteristics of the phenomena that must be monitored. In view of the advantages of slow scanning, the data update rate in an air weather surveillance radar need be no faster than that dictated by the temporal and spatial parameters of hazardous atmospheric features. This establishes a need for a thorough study of the lifetimes of hazardous atmospheric phenomena.

Data Base for the Study

The data for the present study were collected using NSSL's Doppler radar facility at Norman, Okla. The main parameters of the radar during data collection are listed in Table 1. The pulse pair processor provides data consisting of three moments—reflectivity, radial velocity, and Doppler spectrum width—at each resolution cell in the scan volume.¹³ The NEXRAD will have a similar capability.

The current study utilizes data collected during the spring seasons of 1980 and 1981 using the scan patterns shown in Fig 4. The scan elevation levels were occasionally varied depending on the distance of the storm from the radar.

Lifetime Estimation by Photointerpretation

Background

A photographic study of the evolution of a storm field with time provides a simple and direct way of estimating feature lifetimes. This method was employed in the initial stages of our study. The photographs were obtained from the versatile

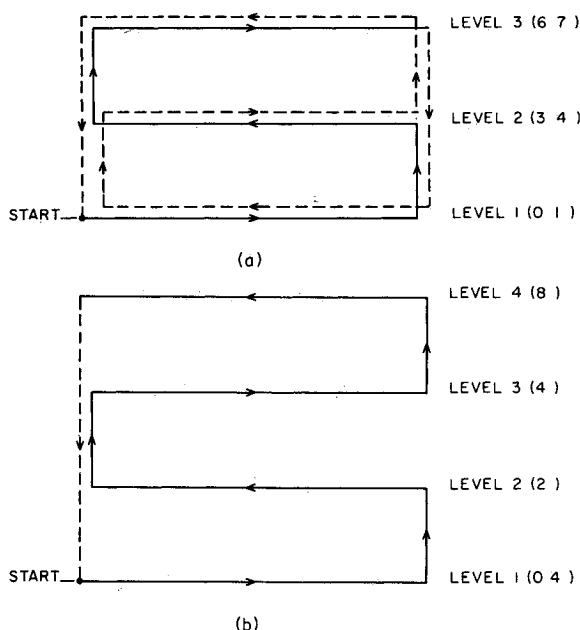


Fig 4 Scan cycles for data collection during a) 1980 and b) 1981. The sector widths are variable. The elevation angles corresponding to scan levels were also occasionally varied.

Table 1 Radar parameters during data collection

Parameter	Value/status
Half power beamwidth	0.8 deg
Antenna gain	46.8 dB
First side lobe level of antenna	21 dB
Polarization	Vertical
Scan rate	8 deg/s
Wavelength	10.52 cm
Pulse repetition time	768 μ s
Pulse width	1 μ s
Peak power	750 kW
Receiver 3 dB bandwidth	1.2 MHz
Processing	Pulse pair based on 64 samples

and high-quality color PPI displays for spectral moments, developed and operating at NSSL. Each of the three spectral moments is quantized to 16 levels, and each level is represented either by a separate color or a shade of gray. The resulting display for each moment is a color or shaded black and white field giving a pictorial presentation of the various phenomena and features within the field.

For the purpose of this study, significant features are defined as those with one or more of the following attributes: 1) reflectivities exceeding 40 dBZ, 2) velocities in local areas exceeding 20 m/s (approximately 40 knots) and 3) Doppler spectrum widths exceeding 4 m/s. Such features may either pose a potential hazard to aviation or cause discomfort in flight. The basis of the reflectivity threshold is a set of measurements in the mid 1970s that indicate that moderate or severe turbulence can be expected somewhere in a storm complex when the maximum reflectivity factor is 40 dBZ or

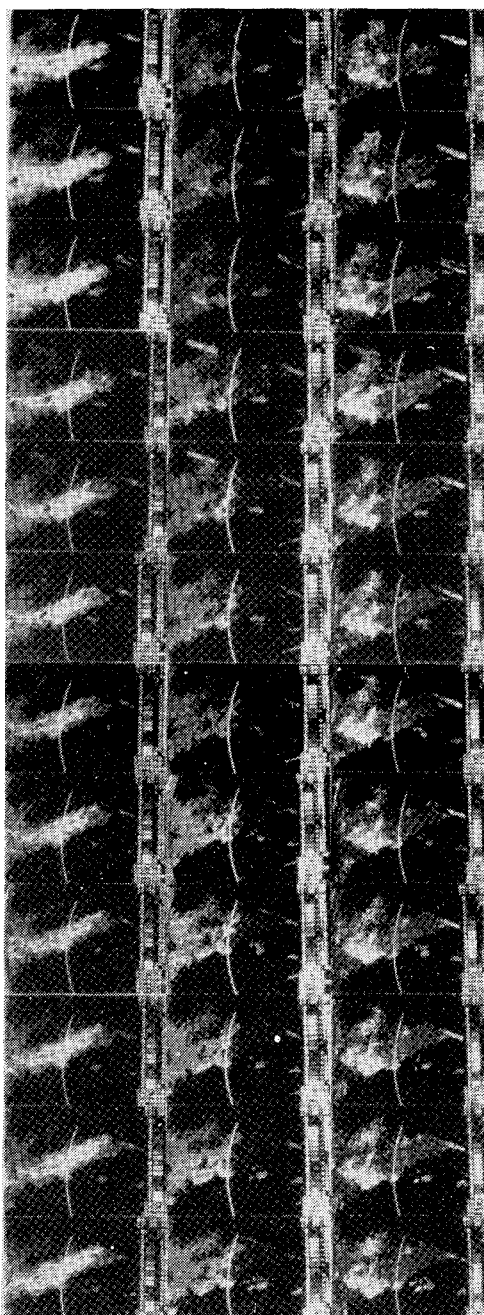


Fig 5 Spectral moment displays of a storm that occurred on April 24, 1980. The scan elevation was 0.4 deg. The left, center, and right columns, respectively, show the evolution of reflectivity, radial velocity, and spectrum width with time.

higher.¹⁸ Also, spectrum widths were examined vis-à-vis the turbulence encountered by aircraft penetrating storms. In all cases of moderate or severe turbulence, the spectrum width was found to be in excess of 4 m/s (Ref. 18). This explains the threshold on the Doppler spectrum width. Such definite quantitative relationships between peak radial velocities and aviation hazards are not available. Large areas of nearly uniform windspeed do not appear to be detrimental to flight even for fairly high values of wind speed. This is because the pilot would have sufficient time to adjust control surfaces to compensate for drift within a large mass of moving air. Windshear, however, has a strong potential for aviation hazard, particularly when occurring at lower levels. Thus, localized pockets of high wind speeds would be a cause of concern. Since shear is difficult to measure directly, we have chosen instead a threshold of 20 m/s (approximately 40 knots) on local radial velocity peaks as a hazard indicator.

Five storms were studied using the photographic method. These storms occurred on April 24, June 16, and June 17 of 1980, and April 3 and April 19 of 1981. Data on these storms suitable for lifetime studies are available over a period of 10–12 min. This period is adequate, since the intention is to find if there are any features with lifetimes less than the order of 5 min. Features persisting over periods greater than 10 min will have no difficulty in being detected.

Observations

As a representative set, a sequence of photographs obtained from the April 24, 1980, storm are reproduced in Fig. 5. The photographs were originally obtained in color but are reduced to a compact black-and-white set here for ease of reproduction. This process, however, necessarily involves some loss of information and, less importantly, of appearance and clarity. The sequence in Fig. 5 was obtained at an elevation angle of 0.4 deg. Similar sequences are available for other scan levels of the same storm as well as for the several scan levels of each of the other storms. The full set of photographs and detailed discussions on individual features are provided elsewhere.¹⁹ The main findings are summarized here.

An analysis of the photographic sequences shows that most of the significant features in these storms, including those of relatively small spatial extent, remain quite stable and recognizable. Occasionally, individual features at certain scan levels exhibit somewhat rapid growth in strength and extent. This may be explained by the fact that thunderstorm activity usually starts at midaltitudes and rapidly propagates both upward and downward. Thus, at a level just above or below the storm nucleus, a rapid growth in area and severity of the feature would be noticed. However, if data from several levels of scan are superimposed, such phenomena would not escape detection.

In some situations, the internal details of a feature may undergo considerable change during the observation period, though the approximate extent and location, as well as the highest value of the moments within the feature, remain nearly unchanged. From the aviation point of view, such features are considered to be persistent, since a safe ATC procedure encourages aircraft to skirt entire storm areas rather than steer through narrow lanes between convective air masses.

Lifetime Estimation by Correlation

Basis of the Method

Correlation is an established way of finding the “amount” of similarity between two fields of statistical data. When the two fields consist of dissimilar parameters and/or have no a priori commonality of origin, the process of correlation is called cross correlation and is utilized to find the relationship between the two fields. Autocorrelation, in contrast, is performed between two fields having an evolutionary

relationship, i.e., one of the fields evolves from the other in time, space, or both. A major difference between autocorrelations and cross correlations is that the autocorrelation coefficient always reaches a maximum value of unity (corresponding to the beginning of evolution, when the two fields are identical) whereas the cross correlation coefficient does not necessarily approach that value.

The correlation coefficient ρ_{xy} between two fields of random numbers $X\{x_i, i=1, \dots, M\}$ and $Y\{y_i, i=1, \dots, M\}$ is defined as

$$\rho_{xy} = \frac{1}{M} \sum_{i=1}^M (x_i - \bar{x})(y_i - \bar{y}) / (\sigma_x \sigma_y) \quad (4)$$

where \bar{x} , \bar{y} are the mean values of the sets X and Y ; σ_x , σ_y are the standard deviations of the sets X and Y ; and M is the number of samples in each set. The correlation coefficient equals unity either when the sets X and Y are identically equal or when each member of one set may be obtained by multiplying the corresponding member of the other set by a constant, i.e.

$$\rho_{xy} = 1 \quad (5)$$

for

$$x_i = k y_i \quad (6)$$

where k is a scalar constant.

The correlation method is a potent tool for studying the evolution (growth and decay) of weather phenomena. This is so because the correlation coefficient, which measures the similarity between fields, may be used to determine how much of the original characteristics are retained by a section of a weather field with lapse of time. The method works as follows:

1) To study the rate of decay, an instant is chosen before the start of rapid decay, and the state of the weather field at that instant is taken as the reference or zero lag field.

2) The parameter to be correlated is selected to be either reflectivity, velocity, or spectrum width.

3) A series of later instants, typically a minute to a few minutes apart, are chosen, and the states of the field at these instants are called lag fields.

4) The successive lag fields are correlated, one at a time, with the reference field, and the correlation coefficient is plotted as a function of time. The general shape of such a curve is a decreasing exponential; its rate of decay corresponding to that of the phenomenon under investigation. The time taken by the correlation coefficient to fall below a suitable threshold value is a quantitative measure of the decay rate of the features contained within the field.

5) To study the rate of growth of weather fields, the fully grown field should be used as the reference, and correlation with successive fields should be performed with lags taken backward in time. Again, the growth period may be defined as the interval during which the correlation coefficient stays above a suitable threshold.

6) The total lifetime of a feature is the sum of the growth period, the stable period, and the decay period.

Description of the Correlation Procedure

Starting from the data stored on tapes, three programming stages are involved in determining feature lifetime by computer correlation: 1) raw data editing, 2) data interpolation, and 3) correlation. An initial process of editing is necessary to "clean up" the raw data that may be contaminated from several sources, chief among which are noise and echo overlaying. The editing program identifies those points (resolution cells) in the data field where the signal-to-noise ratio is too poor for the data to be reliable. The data at such points are deleted, and a marker is set up to identify these points during later processing. The editing program also performs range unfolding wherever possible and discards the points at which range ambiguity cannot be resolved.

Raw Doppler data are collected and stored at discrete azimuthal increments of the order of a beamwidth. These increments vary considerably. Also, azimuth sampling is not synchronized from scan to scan, so that the data grid corresponding to scans at different times are not coincident. This feature is retained even after editing, since editing is performed on a radial by radial basis. To minimize errors that may arise from the use of a nonuniform and noncoincident data grid, an interpolation process is performed to reduce the data from all scans to a standard grid.

The significant operations in the correlation program are shown in the flowchart on Fig. 6. The program can simultaneously handle a number of features. A mapping facility is provided to obtain a printout of the moment field of interest. This helps in the selection of features for lifetime study. The geometry of the correlation process is shown in Fig. 7. The essential operation is to move the feature boundary over a limited range and azimuth about the expected position of a feature in a delayed field and correlate each of these positions with the feature in the original field in an

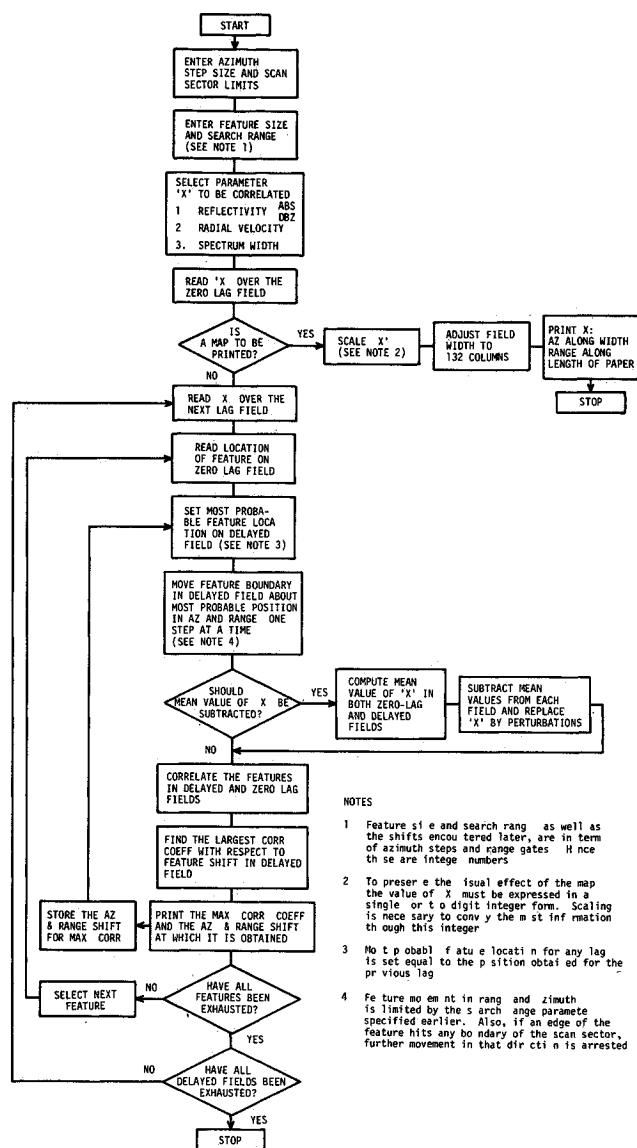


Fig. 6 Simplified flowchart for the determination of maximum correlation coefficient of each of several features at each of several time lags

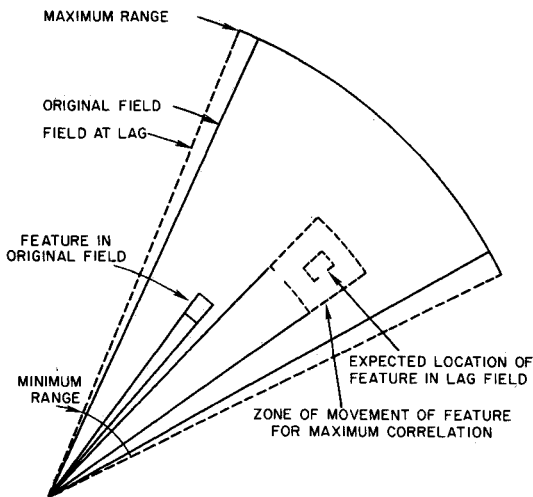


Fig 7 Geometry of the feature correlation process

attempt to find the maximum value of correlation coefficient. This maximum value is plotted as a function of time lag.

Results

The correlation time plots provide information on the lifetimes of features. A best fitting curve in a least squares sense is drawn through the points in each plot to show the trend and to obtain a numerical value for the decay rate of the correlation coefficient. For most natural decay phenomena, the decrease of the correlation coefficient with time is expected to follow an exponential law of the type

$$\rho_{xy}(t) = \rho_{xy}(0^+) \exp(-\beta t) \quad (7)$$

where $\rho_{xy}(t)$ is the maximum correlation coefficient between the zero lag field and the field at time lag t ; $\rho_{xy}(0^+)$ is the maximum correlation coefficient between the zero lag field and the field configuration slightly later; and β is the time constant of the decay. Although the correlation coefficient $\rho_{xy}(0)$ of a field with itself is unity by definition $\rho_{xy}(0^+)$ would, in general, be less than unity because of the presence of white noise.

Equation (7) is based on the assumption that the steady state value of the correlation coefficient is zero. However, because of the presence of phenomena of different scale sizes, the actual decay law would be a superposition of many exponentials of the type given by Eq (7). Thus, over a limited period such as the 10 or 12 min interval for which lifetime data have been collected and analyzed, the decay curve may appear to settle down to a nonzero steady-state value. Such a tendency was observed in many of the graphs obtained from the computer aided correlation procedure. To account for such behavior, the following modified form of Eq (7) was used to obtain the best fitting curve for the computed correlation coefficients:

$$\rho_{xy}(t) = \rho_{xy}(\infty) + [\rho_{xy}(0^+) - \rho_{xy}(\infty)] \exp(-\beta t) \quad (8)$$

Here, $\rho_{xy}(\infty)$ is the steady state value of the correlation decay curve. It may be noted that Eq (8) is a more general form that reduces to Eq (7) if $\rho_{xy}(\infty)$ is assumed to be zero. Thus, if Eq (7) is indeed the best fit for a particular set of points in preference to Eq (8), the optimization program that minimizes the rms error would automatically select Eq (7) by assigning zero to the steady state value.

Before proceeding to present the results of computation it is necessary to establish a way of interpreting the correlation

history curves to obtain a quantitative measure of lifetimes. This in turn requires an understanding of the significance of the three parameters of curve fitting, namely $\rho_{xy}(0)$, β , and $\rho_{xy}(\infty)$. The first of these may be interpreted as the true autocorrelation of the feature at zero lag; i.e., white noise effects are isolated. Thus, the more the noise content in the observations, the more will $\rho_{xy}(0^+)$ fall short of unity. To obtain a quantitative estimate of lifetime it appears logical not to set an absolute threshold, but a threshold that is a fraction of $\rho_{xy}(0^+)$. At this point, a certain amount of arbitrariness is inevitable. We measure lifetime of a feature as the interval during which the maximum correlation coefficient curve as a function of time, remains above $0.5 \rho_{xy}(0^+)$.

The other two parameters, i.e., β and $\rho_{xy}(\infty)$ depend on the relative scales of structures within the feature being correlated. A larger value of β , corresponding to faster decay, usually signifies a strong fine structure within the feature. On the other hand, a large residual or steady state correlation $\rho_{xy}(\infty)$ indicates the presence of significant large scale structures. Thus, the correlation history curves provide more information regarding the evolution of each feature than a single number signifying its lifetime.

A brief discussion is in order here on the choice of features for correlation. It would be ideal to study each individual cell within the storm, but automatic recognition and location of the center and boundary of each cell is a highly involved problem by itself and has not been attempted here. Instead, feature selection is done by looking at a computer printout of the moment field. For simplicity, a "rectangular" feature shape has been used, i.e., the feature is bounded between two radials and two range circles. The features have been generally so chosen as to include a peak (which may be local) in at least one of the moment fields. However, consideration has also been given to their "trackability," i.e., the presence of distinct characteristics, such as significant two dimensional gradients or variations, etc. Not all the features discussed in the following paragraphs are significant in the sense of the three criteria laid down earlier; however they have been included to increase the statistical base available for this study. The assumption here is that there is no fundamental statistical difference between strong and somewhat weak features.

The results of computer correlation of April 24, 1980, storm Doppler data are presented in Fig 8. The radial lines are interpolated to a grid at 0.5 deg intervals. A feature is taken to extend over 20 range gates and 20 radials, which translates to 3 km \times 10 deg in spatial coordinates. Figure 8a corresponds to a scan elevation of 0.4 deg. Six features are studied and the correlation history of all the three moments (corresponding to reflectivity, radial velocity, and Doppler spectrum width) are shown. Several observations can be made from this set of graphs:

1) Different features within the same storm can have widely differing range of correlation values. For example, in Fig 8a, reflectivity correlation coefficients for feature 2 lie between 0.25 and 0.54, whereas those for feature 5 remain consistently above 0.87 during the period of observation.

2) In the reflectivity field, features with large reflectivity values and gradients generally have higher correlation values than those with small peak reflectivities and weak gradients. As an example, the peak reflectivities of features 1, 6 in Fig 8a are 23, 26, 35, 58, and 61 dBZ, respectively. Here, although small increments in peak reflectivities do not necessarily result in a corresponding increase in correlation, as between the first and second features, the last three features, which have very high peak reflectivities, have a much higher average correlation level than the first three. A high reflectivity level contributes to high correlation by minimizing the noise contribution to the shortfall of the correlation coefficient from unity. A high reflectivity gradient within the field causes larger departure of individual cell reflectivities from the feature mean. Large departures further minimize the effect of

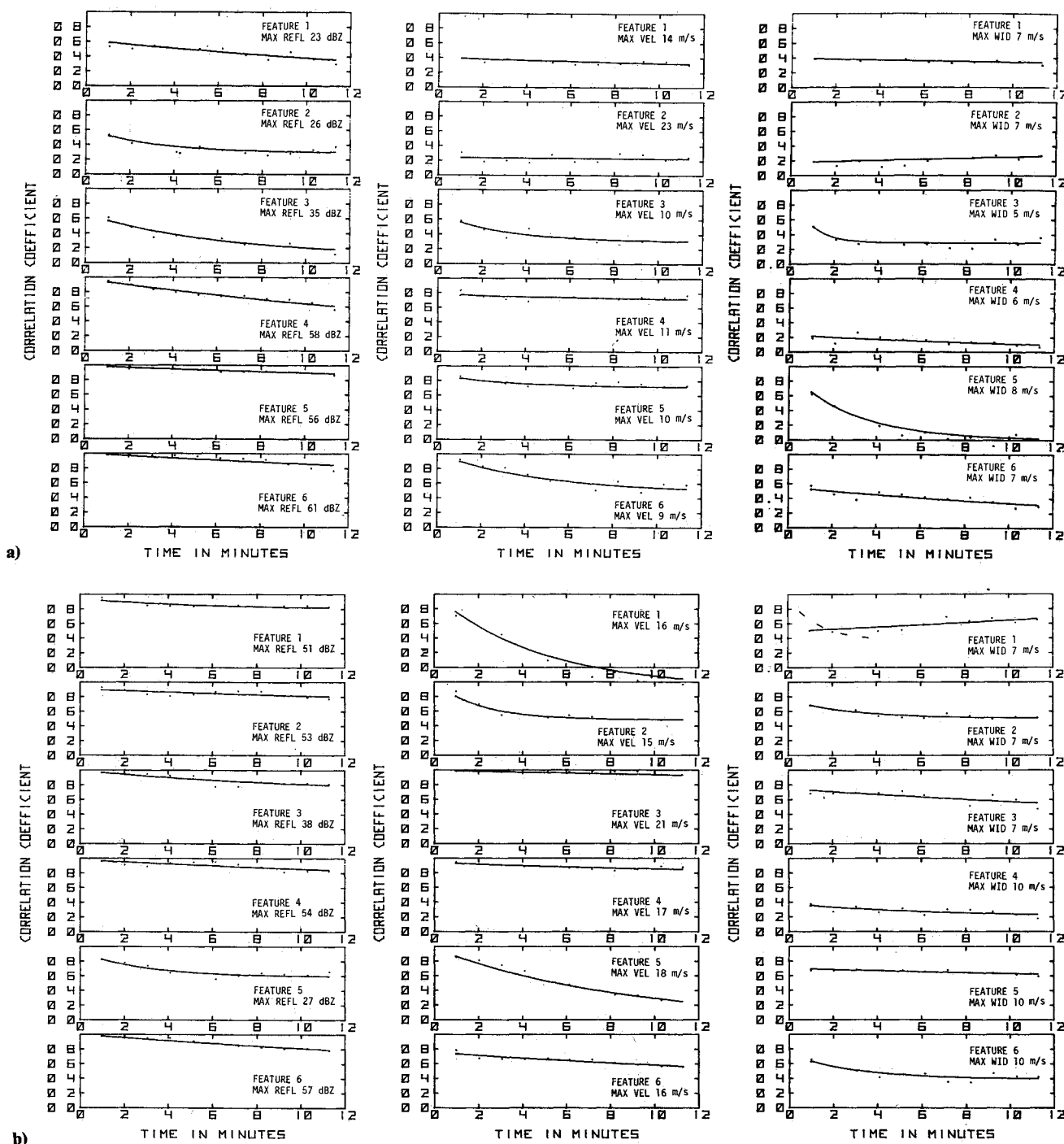


Fig 8 Correlation evolution of April 24 1980 storm at elevation angles of a) 0.4 deg and b) 3.5 deg. The left column is for reflectivity, the center column for velocity, and the right column for spectrum width. Range to storm center is about 40 km.

noise and, because of longer persistence, increase long term correlation as well.

3) The correlation values in most cases decrease from reflectivity field through velocity field to the spectrum width field. This signifies that the noisiness in the field increases with the order of the moment. However, it is not clear how much of this noise is due to the high frequency meteorological variations and how much comes from the spectral moment estimation uncertainties. But, based on the signal to noise ratios normally encountered for echoes from storms and the behavior of estimators, we believe that the larger contribution should come from the first source. We note here that in a previous study⁷ of clear-air phenomena the strongest correlation was associated with the velocity field. Several

factors could contribute to such a discrepancy. Most important among these is that the reflectivity and velocity gradients within the feature are not always correlated, i.e., large reflectivity variations do not necessarily imply large velocity variations and vice versa. Since strong parameter variations tend to yield large correlation coefficients, the relative values of reflectivity and velocity (also spectrum width) correlation may vary from case to case. The origins of reflectivity in storms and clear air are different. In storms precipitation, which is the source of reflectivity, may have relatively strong gradients and a large dynamic range. In clear air reflectivity arises from fluctuations in refractive index and from insect populations. Local changes in reflectivity are caused by variations in humidity and insect concentrations,

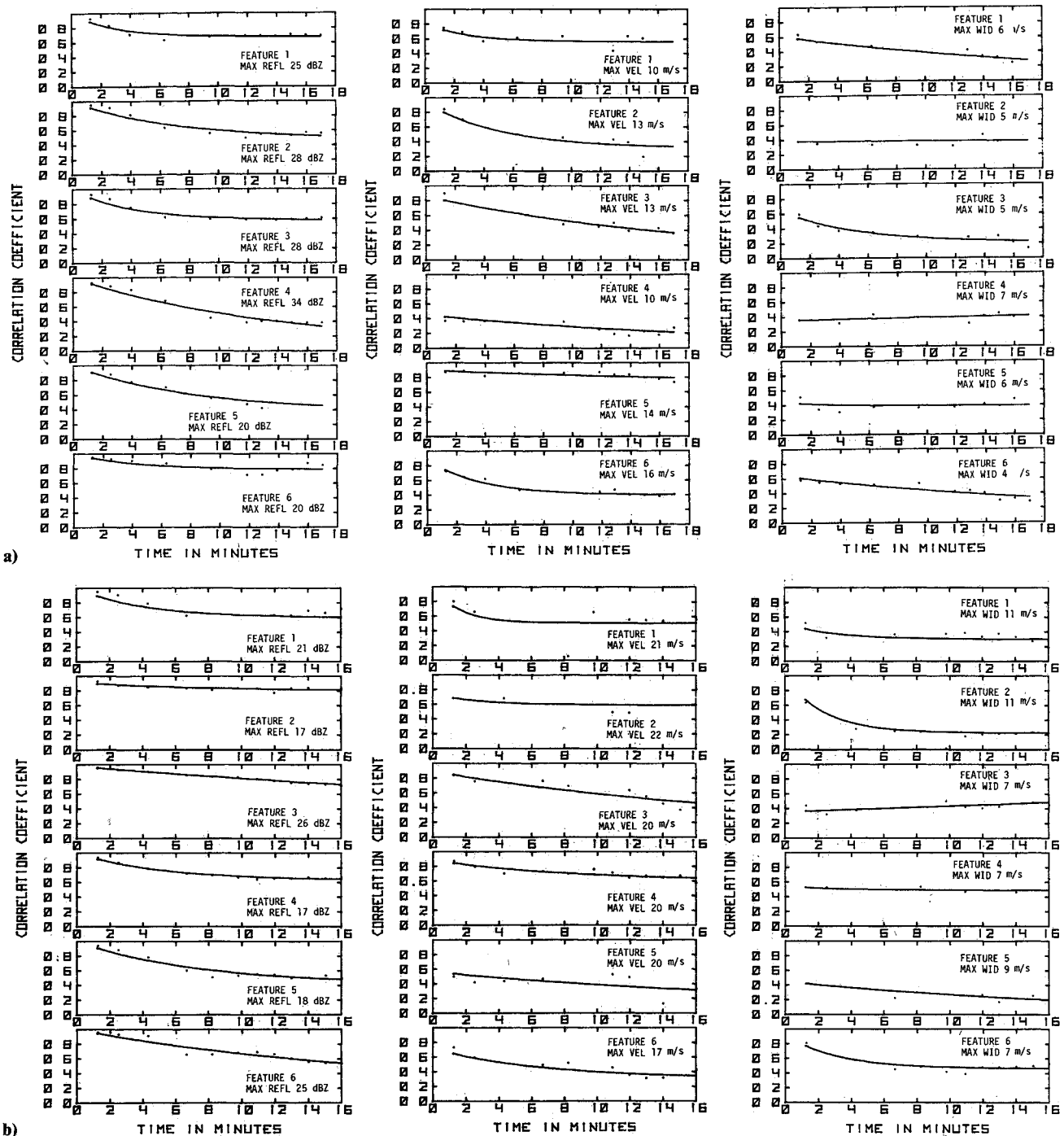


Fig 9 Correlation evolution of June 17, 1980 storm at elevation angles of a) 0.8 deg and b) 1.8 deg The left column is for reflectivity, the center column for velocity, and the right column for spectrum width The storm complex had features distributed from the radar site out to over 120 km

but these variations are usually gradual, resulting in weak reflectivity gradients. A second factor explaining the discrepancy is that since clear air reflectivities are low (<10 dBZ) compared to storms (up to 70 dBZ), the estimation uncertainties due to receiver noise are larger in the case of clear air. Estimation uncertainties act as white noise and decorrelate at all time instants except $t=0$. Clearly, further research and intercomparison of the correlation fields are in order.

4) The lifetimes of features can vary substantially depending on which field is used to estimate it. As an extreme example, in Fig 8a judging by the reflectivity and velocity fields, feature 5 has a lifetime well above the 12 min observation period, but, based on spectrum width, its lifetime is of the order of 3 min. This observation leads to the caution

that aviation weather surveillance should be carried out using all three spectral moments to improve the chance of detection.

5) All six features have lifetimes greater than 5 min, in at least one moment field.

Figure 8b shows correlation results for middle elevation levels, 3.4 to 3.6 deg. These results support observations at lower levels. The reflectivity map at this elevation shows heavy precipitation, exceeding 40 dBZ, over extensive areas and 50 dBZ in several places, and, hence, the reflectivity correlation of all features at this elevation shows high values. The velocity field shows a lot of diversity. The velocity correlation of the first feature shows rapid decay, with a lifetime of about 3 min. However, in the other two fields, i.e., reflectivity and spectrum width, the feature shows high persistence, well in excess of 12 min. The same is true of

feature 5, though the difference between its lifetimes in the velocity and the other two fields is less dramatic. From the three sets of graphs in Fig 8b the observation is again made that in at least one of the moment fields, each feature has a lifetime exceeding 5 min.

A discussion is in order here regarding the anomalous behavior of the spectrum width correlation of feature 1 in Fig 8b. Such behavior may be caused by one or a combination of two factors: 1) statistical uncertainties and 2) the internal structure of the feature. If the feature contains a strong fine structure, i.e., rapid small-scale variations, such variations would die out or rearrange themselves relatively quickly, causing the maximum correlation coefficient to drop rapidly initially. This appears to be true if one considers the first three data points in the graph, which have been manually joined by a broken line to show the trend. After the maximum correlation coefficient has fallen sufficiently, spurious correlation peaks begin to compete with it. If a spurious peak exceeds the true peak, the correlation program loses track of the "original" feature and switches over to the location of the spurious peak. However, since the part of the field that caused the spurious peak is uncorrelated to the original feature, once the original feature is lost, the program will jump from one spurious peak to another (always settling for the highest peak in the vicinity of the previous peak), thus presenting an erratic behavior on the correlation evolution graph. Such a random string of points has a significant probability of showing an increasing trend. Loss of track of the original feature may be made less frequent by building more complexities into the correlation program that recognize and follow more attributes of a feature than just the correlation coefficient. Such finer aspects have not been included in the present work.

The results for the high level scan at 7 deg (plots not shown) are in general agreement with the observations made earlier, although the precipitation at this elevation was weak (maximum reflectivity, 31 dBZ). Because of lower reflectivity, the reflectivity correlation coefficients are smaller than those corresponding to the lower two elevations. Also, the scatter of points is larger due to relatively higher noise effects. The lifetimes of all five features observed at 7 deg elevation are longer than 5 min.

The stability of features at two scan levels, 0.8 and 1.8 deg, of the June 17, 1980 storm is represented by the sets of graphs in Figs 9a and 9b, respectively. Six features have been considered at each elevation, and correlation has been performed for each feature in all the three moment fields. The results show that each feature at each elevation in this storm persists over 5 min.

Correlation results for a storm that occurred in central Oklahoma on April 3, 1981, further corroborate the above findings. Each of the several features considered in this storm was found to have a lifetime far in excess of 5 min. The velocity field of this storm exhibited some apparently anomalous behavior, a discussion of which is necessary to bring out one of the weaknesses of the correlation method. Figure 10a shows the correlation evolution of the radial velocity fields of six features in this storm at 0.4 deg scan elevation. Although the wind field was quite extensive and strong, reaching radial speeds of 23 m/s, the correlation coefficients in Fig 10a are seen to be rather low. This behavior may be traced to the relative uniformity of the wind field. When the value of the parameter being correlated has a small range of variation over the entire feature, irrespective of the actual parameter value, its perturbation over the mean is small. This has the effect of amplifying the relative contribution of the basic measurement uncertainty to the correlation coefficient. Since the uncertainty acts as white noise, the correlation coefficient at all delays but zero tends to be small. To test this hypothesis, correlation coefficients were computed for three large features, each extending over 60 range gates and 50 radials (9 km \times 25 deg). The results are

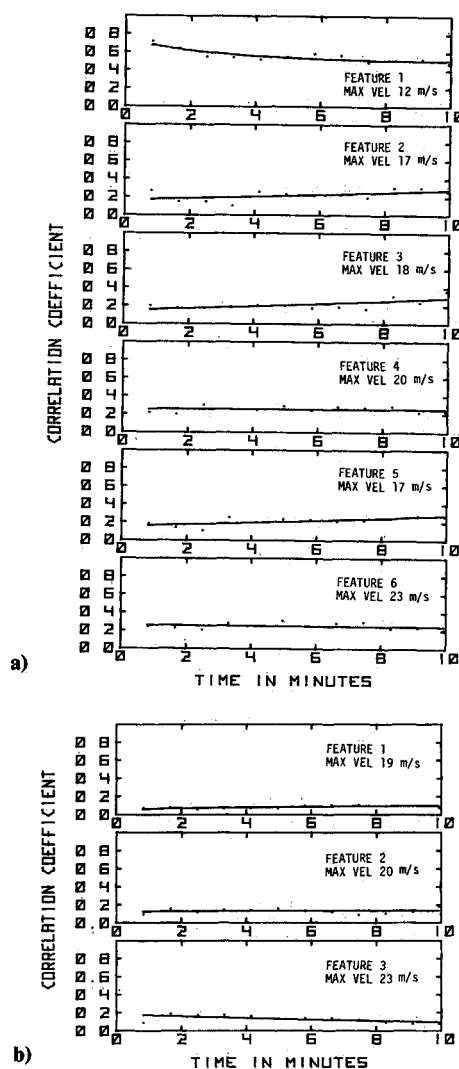


Fig 10 Correlation evolution of the radial velocity field of April 3, 1981 storm at 0.4 deg scan elevation. Part a) shows the results for six features, each 3 km \times 10 deg, and part b) for three large (9 km \times 25 deg) features. Range to storm center is approximately 60 km.

shown in Fig 10b. When a large number of points in a white noise process are correlated, the central spike (or delta-function located at the origin) becomes sharper, and the scatter of correlation values is expected to be reduced. The graphs of Fig 10b do indeed show such a behavior, with low, nearly uniform correlation away from origin and greatly reduced scatter in comparison with Fig 10a.

Limitations of the Method

From previous discussion, the correlation method, when used alone, appears to have a disadvantage in tracking and estimating the lifetimes of features in a large, nearly uniform field. One way to minimize this problem is to assume feature boundaries well outside the flat portion of the field. However, this may result in feature sizes that are very large, leading to loss of resolution and large computational requirements. Also, since larger features tend to persist longer, very large features are not likely to resolve the question of whether the data update rate should be 5 min or 2.5 min; they would probably always last much longer than 5 min.

The correlation procedure, as used in this study, has a few shortcomings. Among these are the following:

1) No automatic feature identification capability has been built into the program. Automatic feature identification is an involved problem by itself and is being solved elsewhere.^{20,21} In principle, such an algorithm can be coupled to the

correlation procedure. However, automatic detection has not been found essential to this program, since the lifetime algorithm is not meant for operational implementation or air traffic control purposes but is intended to generate statistics which may be done off line.

2) It is assumed that features merely translate in a polar coordinate, in addition to undergoing internal changes. Other possible motions, such as rotation, shear stretching, etc., are ignored. This is done to keep the problem tractable. However, this does not adversely affect the conclusions of the present study, since the lifetime estimates tend to be conservative on the lower side; i.e., inclusion of rotation, etc., would make the features appear more persistent and hence, more easily detectable.

Concluding Remarks

The lifetimes of the significant features in several central Oklahoma storms have been studied in this report using photo-interpretation and computer aided time-lapse correlation. The motivation for this study was to generate data that would help decide whether an update rate of once in 5 min would be adequate for en route aviation weather surveillance using NEXRAD, or whether it would be necessary to renew information every 2.5 min so that if there are fast transient phenomena, they would not be missed by falling between scan cycles. Storm data from 1980 and 1981 spring programs have been used in this study, and a scan interval less than 2.5 min has been used for each storm observation.

The clear observation from both the photo interpretive and correlation studies is that, among the storms examined, there is no significant or potentially hazardous change in any feature that would be missed by a 5 min cycle. There are isolated scan levels and moment fields in which certain features appear to grow or decay within time scales faster than 5 min. However, if observations from several scan levels and all the three moment fields (reflectivity, radial velocity, and Doppler spectrum width) are properly combined, then this study provides overwhelming evidence that a simple, monotonic, 5-min scan should be adequate for application of NEXRAD to en route air weather surveillance.

To conclude beyond all reasonable doubt that ultrafast convective phenomena are so rare as not to affect NEXRAD scan strategy, one would have to study a large number of storms over an extended period of time. This report is based on data from five storms taken during two spring seasons, those of 1980 and 1981. While the assumption is that these storms are representative, it is possible that the set is atypical. Further, no attempt has been made to explicitly identify hazardous phenomena such as tornadoes, downbursts/microbursts, hail, etc., because of the lack of independent confirmation, although these may have been present within the storms examined. Thus, further data collection, processing, and interpretation to corroborate the findings in this report are in order. Although some of our findings, such as persistence of high reflectivity areas and turbulent patches, may be applicable to airspace at the terminal area, data on the low-level windshear were not available. At our lowest elevation (0.4 deg), the beam center was about 400 m above ground for the closest storm. Therefore, if shallow downbursts were present, their divergent flow near ground would not have been detected. At present, downburst precursors are not understood, so there are no known procedures to detect them. Because 50% of microbursts' outflow reaches maximum in less than 5 min from first detection, update rates for reliable detection may have to be about 2 min (Ref. 22).

Most of the data used in this study were collected during the period when the storms had already stabilized. This has been due to the very nature of the data collection process. Thus, the explosive growth and, less importantly, the rapid decay

periods of the storms have not been considered. This is a limitation of this study. Very sharp rainfall growth rates have been predicted by certain models²³ but do not appear to have been substantiated by observations.

However, there is reason to believe that the conclusions of this report would not be changed very much if and when data on the explosive growth periods are included in the study. Experience has shown that large jumps in reflectivity usually occur over pre-existing cells of detectable strength. Furthermore, if such growth of precipitation is to occur, it must be preceded by vigorous dynamical processes in the cells that should be detectable in the velocity and/or Doppler spectrum width fields if not the reflectivity field.

Acknowledgment

This work was sponsored by the Federal Aviation Administration under Contract DTFA01 80 Y 10524. The authors acknowledge the numerous discussions with R. J. Doviak, Chief of Doppler Radar and Storm Electricity Research at NSSL, which yielded valuable insight into the problem. P. R. Mahapatra was a research associate of the National Research Council while this study was conducted. Michelle Foster typed the manuscript and Joan Kimpel helped in preparing the illustrations.

References

- ¹Lerner, E. J., 'Automating U.S. Air Lines: A Review' *IEEE Spectrum*, Vol. 19, Nov. 1982, pp. 46-51.
- ²NEXRAD Joint System Program Office, 'Next Generation Weather Radar Research and Development Plan', Dec. 1981.
- ³Blackmer, R. H. Jr., 'The Lifetime of Small Precipitation Echoes', *Proceedings Fifth Weather Radar Conference and 139th National Meeting of the AMS*, Asbury Park, N. J., Sept. 12-15, 1955, pp. 103-108.
- ⁴Rinehart, R. E., 'Internal Storm Motions From a Single Non-Doppler Weather Radar', National Center for Atmospheric Research, Boulder, Colo., Technical Note NCAR/TN-146+STR, Oct. 1979.
- ⁵Wilson, J. W., 'Movement and Predictability of Radar Echoes', National Severe Storms Laboratory Technical Memo IERTM NSSL 28, Nov. 1966.
- ⁶Kessler, E. III and Russo, J. A. Jr., 'Statistical Properties of Weather Radar Echoes', *Proceedings of the 10th Weather Radar Conference*, Washington, D.C., April 22-25, 1963, pp. 25-33.
- ⁷Smythe, G. R. and Zrnic, D. S., 'Correlation Analysis of Doppler Radar Data and Retrieval of the Horizontal Wind', *Journal of Climate and Applied Meteorology*, Vol. 22, Feb. 1983, pp. 297-311.
- ⁸National Transportation Safety Board, *Annual Review of Aircraft Accident Data: U.S. Carrier Operations* (published annually).
- ⁹National Transportation Safety Board, *Briefs of Fatal Accidents Involving Weather as a Cause/Factor: U.S. General Aviation* (published annually).
- ¹⁰Bromley, E. Jr., 'Aeronautical Meteorology: Progress and Challenges—Today and Tomorrow', *Bulletin of the American Meteorological Society*, Vol. 58, Nov. 1977, pp. 1156-1160.
- ¹¹Lee, J. T. and Wilk, K. E., 'Applications of Conventional and Doppler Radars for Aviation Safety', Paper presented at the 19th Conference on Radar Meteorology, American Meteorological Society, April 15-18, 1980, Miami Beach, Fla., pp. 102-109.
- ¹²Fujita, T. T., 'Downbursts and Microbursts—An Aviation Hazard', Paper presented at the 19th Conference on Radar Meteorology, American Meteorological Society, April 15-18, 1980, Miami Beach, Fla., pp. 94-101.
- ¹³Doviak, R. J., Zrnic, D. S., and Sirmans, D. S., 'Doppler Weather Radar', *Proceedings of the IEEE*, Vol. 67, Nov. 1979, pp. 1522-1553.
- ¹⁴Zrnic, D. S., 'Estimation of Spectral Moments for Weather Echoes', *IEEE Transactions on Geoscience Electronics*, Vol. GE-17, No. 4, Oct. 1979, pp. 113-128.
- ¹⁵Zrnic, D. S. and Doviak, R. J., 'Effective Antenna Patterns of Scanning Radars', *IEEE Transactions on Aerospace Electronic Systems*, Vol. AES-12, Sept. 1976, pp. 551-555.
- ¹⁶Groginsky, H. L. and Glover, K., 'Weather Radar Cancellor Design', Paper presented at the 19th Conference on Radar

Meteorology American Meteorological Society Boston Mass , April 1980 pp 192 201

¹⁷Zrnic' D S and Hamidi S 'Considerations for the Design of Ground Clutter Cancelers for Weather Radar U S Department of Transportation Federal Aviation Administration Report DOT/FAA/RD 81/72 Feb 1981

¹⁸Zrnic , D S and Lee, J T , Pulsed Doppler Radar Detects Weather Hazards to Aviation *Journal of Aircraft* Vol 19 Feb 1982, pp 183 190

¹⁹Mahapatra P R and Zrnic D S Scanning Strategies for Next Generation Weather Radars: A Study Based on Lifetimes of Convective Atmospheric Phenomena Hazardous to Aviation U S Department of Transportation Federal Aviation Administration Report DOT/FAA/RD 82/69 July 1982

²⁰Crane R , Automatic Cell Detection and Tracking *IEEE Transactions on Geoscience Electronics* Vol GE 17 No 4 Oct 1979 pp 250 262

²¹Crane R K Radar Analysis for Severe Weather Detection and Tracking U S Department of Transportation Federal Aviation Administration Report DOT/FAA/RD 82/64 July 1982

²²Wilson J and Roberts, R , Evaluation of Doppler Radar for Airport Wind Shear Detection ' Paper presented at the 21st Conference on Radar Meteorology, American Meteorological Society Edmonton Alberta Canada 1983 pp 616 623

²³Yau, M K A Two Cylinder Model of Cumulus Cells and Its Application in Computing Cumulus Transports, *Journal of the Atmospheric Sciences* Vol 37 Nov 1980 pp 2470 2485

From the AIAA Progress in Astronautics and Aeronautics Series

AEROACOUSTICS:

JET NOISE, COMBUSTION AND CORE ENGINE NOISE—v 43

FAN NOISE AND CONTROL; DUCT ACOUSTICS, ROTOR NOISE—v 44

STOL NOISE, AIRFRAME AND AIRFOIL NOISE—v 45

ACOUSTIC WAVE PROPAGATION,

AIRCRAFT NOISE PREDICTION,

AEROACOUSTIC INSTRUMENTATION—v. 46

Edited by Ira R. Schwartz NASA Ames Research Center Henry T. Nagamatsu General Electric Research and Development Center and Warren C. Strahle Georgia Institute of Technology

The demands placed upon today's air transportation systems in the United States and around the world have dictated the construction and use of larger and faster aircraft. At the same time, the population density around airports has been steadily increasing, causing a rising protest against the noise levels generated by the high frequency traffic at the major centers. The modern field of aeroacoustics research is the direct result of public concern about airport noise.

Today there is need for organized information at the research and development level to make it possible for today's scientists and engineers to cope with today's environmental demands. It is to fulfill both these functions that the present set of books on aeroacoustics has been published.

The technical papers in this four book set are an outgrowth of the Second International Symposium on Aeroacoustics held in 1975 and later updated and revised and organized into the four volumes listed above. Each volume was planned as a unit so that potential users would be able to find within a single volume the papers pertaining to their special interest.

v 43—648 pp	6 x 9 illus	\$19 00 Mem	\$40 00 List
v 44—670 pp	6 x 9 illus	\$19 00 Mem	\$40 00 List
v 45—480 pp	6 x 9 illus	\$18 00 Mem	\$33 00 List
v 46—342 pp	6 x 9 illus	\$16.00 Mem	\$28 00 List

For Aeroacoustics volumes purchased as a four volume set \$65 00 Mem. \$125 00 List

TO ORDER WRITE Publications Dept , AIAA, 1633 Broadway, New York, N Y 10019